Performance of a prototype atomic clock based on *lin* || *lin* coherent population trapping resonances in Rb atomic vapor

Eugeniy E. Mikhailov, Travis Horrom, Nathan Belcher, and Irina Novikova*

The College of William and Mary, Williamsburg, Virginia 23187, USA
**Corresponding author: inovikova@physics.wm.edu*

Received November 2, 2009; revised December 1, 2009; accepted December 2, 2009; posted December 3, 2009 (Doc. ID 119355); published February 4, 2010

We report on the performance of the first table-top prototype atomic clock based on coherent population trapping (CPT) resonances with parallel linearly polarized optical fields (*lin*‖*lin* configuration). Our apparatus uses a vertical-cavity surface-emitting laser (VCSEL) tuned to the D_1 line of ^{87}Rb with the current modulation at the ^{87}Rb hyperfine frequency. We demonstrate cancellation of the first-order light shift by the proper choice of rf modulation power and further improve our prototype clock stability by optimizing the parameters of the microwave lock loop. Operating in these optimal conditions, we measured a short-term fractional frequency stability (Allan deviation) $2\times10^{-11}\tau^{-1/2}$ for observation times $1\ \mathrm{s}\leqslant\tau\leqslant20\ \mathrm{s}$. This value is limited by large VCSEL phase noise and environmental temperature fluctuation. Further improvements in frequency stability should be possible with an apparatus designed as a dedicated *lin*‖*lin* CPT resonance clock with environmental impacts minimized.

OCIS codes: 020.1670, 270.1670, 020.3690.

1. INTRODUCTION

In recent decades impressive progress has been made in the development of miniature precision measurement devices (clocks, magnetometers, gyroscopes, etc.) that use atomic energy levels as a reference [1–10]. A promising scheme for all-optical interrogation of a microwave clock transition in chip-scale atomic devices is based on the modification of the optical properties of an atomic medium under the combined action of multiple resonant optical fields. For example, under the conditions of coherent population trapping (CPT), the simultaneous action of two optical fields [as shown in Fig. 1(a)] allows "trapping" atoms in a noninteracting coherent superposition of two long-lived hyperfine sublevels of the ground energy state $|g_{1,2}\rangle$ that, under idealized conditions (isolated three-level scheme, no ground-state decoherence), is completely decoupled from the excited state $|e\rangle$. Such a noninteracting state (usually called the "dark state") exists only when the differential frequency of two optical fields (two-photon detuning) matches the energy splitting of the hyperfine states and leads to a narrow peak in optical transmission—the effect known as electromagnetically induced transparency, or EIT [11]. The linewidth of a CPT resonance depends on the intensities of the optical fields, but it is ultimately limited by the finite interaction time of atoms with light. Since it is possible to obtain CPT resonances as narrow as a few tens to hundreds of Hz [12,13], one can lock a microwave oscillator controlling the frequency difference between two optical fields such that its output frequency is stabilized at the atomic transition frequency $|g_1\rangle-|g_2\rangle$ [14]. Frequency stability of such atomic clocks improves for a high-contrast narrow CPT resonance. Also, minimal sensitivity of the CPT resonance frequency to the experiment environmental fluctuations (such as temperature, laser frequency, and power) is required to ensure long-term stable operation of the clock.

Alkali metal atoms (Cs, Rb, etc.) are well suited for practical realization of CPT-based atomic clocks, since their ground electronic state consists of two long-lived hyperfine states. Also, their optical transitions are easily addressable with diode lasers, allowing potential miniaturization of such clock devices. However, the complex Zeeman structure of these atoms poses several challenges. Only the frequency between magnetic field-insensitive Zeeman sublevels $m_F=0$ ("clock transition") of each ground state should be measured to avoid the detrimental effects of ambient magnetic fields, since good magnetic shielding is not likely possible in a chip-scale atomic clock. At the same time, for a traditional CPT configuration using two circularly polarized optical fields, most atoms are concentrated at the magnetic sublevels with the highest angular momentum $m_F=\pm F$ [15] ("pocket" states). As a result, only a small fraction of atoms contribute to enhancing transmission at the clock transition, leading to a very low CPT contrast and consequently to a limited clock stability. Various groups proposed a number of techniques to improve the CPT resonance characteristics [16–19], although many of them add to the complexity of the experimental setup by requiring, for example, two optical fields of different polarizations.

Recently, a promising approach to produce high-contrast CPT resonances with a single phase-modulated laser was proposed [20], taking advantage of a unique level combination of the alkali atoms with nuclear spin $I=3/2$. In general, two optical fields of the same linear polarization (*lin*‖*lin* configuration) do not create the dark

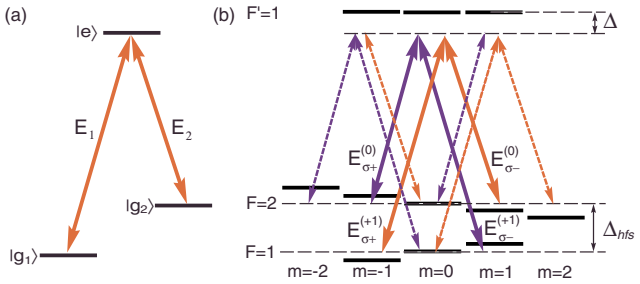

Fig. 1. (Color online) (a) Idealized three-level Λ system that allows for coherent population trapping. (b) Optical transitions excited during the interaction of two linearly polarized optical fields at the carrier frequency $E^{(0)}$ and the first modulation sideband $E^{(+1)}$ for the D_1 line of ^{87}Rb atoms. In the presence of a longitudinal magnetic field each light field is decomposed into σ_+ and σ_- circular components of equal amplitude. Solid arrows indicate the two Λ systems responsible for magnetic-field-insensitive CPT resonances at the hyperfine frequency (*lin*∥*lin* CPT resonances). One-photon detuning Δ is the frequency difference between the $F=2\rightarrow F'=1$ transition and the unmodulated laser frequency.

state required for CPT resonance between the $m_F=0$ sublevels due to destructive interference of the involved Λ systems. However, when two ground states with total angular momenta $F=1,2$ are coupled only with an excited state with a total angular momentum $F'=1$, a high-contrast magneto-insensitive CPT resonance can be formed using $m_F=\pm 1$ Zeeman sublevels [21–24]. In a vapor cell this situation is realized only for the D_1 line of ^{87}Rb, when the excited-state hyperfine levels are spectrally resolved.

The relevant Λ systems formed by the circularly polarized components of two linearly polarized optical fields are shown in Fig. 1(b). In the linear Zeeman-effect approximation, shifts of $|F=1,m_F=\pm 1\rangle$ and $|F=2,m_F=\mp 1\rangle$ are almost identical. The two-photon CPT resonance for a Λ system formed by the σ_+ component of one optical field (e.g., $E_+^{(0)}$) applied to the $|F=2,m_F=-1\rangle\rightarrow|F'=1,m_{F'}=0\rangle$ transition and the σ_- component of the other optical field ($E_-^{(+1)}$) applied to the $|F=2,m_F=-1\rangle\rightarrow|F'=1,m_{F'}=0\rangle$ occurs at the unshifted clock frequency (i.e., at the hyperfine splitting Δ_{hfs}). The same is true for a symmetric Λ system formed by the opposite circular components. The advantage of the *lin*∥*lin* scheme over a traditional *circ*∥*circ* is the absence of any "pocket" states to "hide" atomic population, resulting in a higher-contrast CPT resonance. In addition, the magneto-insensitive CPT resonance in the *lin*∥*lin* configuration is the strongest due to the symmetry of the interaction scheme. CPT resonance contrast up to 25%–35% has been previously demonstrated using a phase-modulated external cavity diode laser [20,24] compared to a few percent for the traditional circular case [1–5].

In this manuscript we report the first experimental realization of a table-top atomic clock prototype based on a *lin*∥*lin* CPT resonance in ^{87}Rb using a VCSEL laser with direct current modulation. Our system is potentially scalable to miniature applications. We demonstrate the cancellation of the first-order light shift of a CPT resonance, confirming the previous results, obtained with an externally phase-modulated narrowband diode laser [24]. Operating in such light-shift-cancellation conditions, we observed promising short-term frequency stability ($\approx 2\times 10^{-11}\tau^{-1/2}$). The long-term stability is limited by insufficient temperature control of the environment. We expect that superior frequency stability will be possible in a small *lin*∥*lin* CPT clock designed for good thermal control, low phase noise, etc.

2. EXPERIMENTAL SETUP

A schematic of the experimental apparatus is shown in Fig. 2. We used a temperature-stabilized vertical cavity surface-emitting diode laser (VCSEL) operating at 794.7 nm (Rb D_1 line). The laser wavelength was locked to the desired atomic transition using a dichroic-atomic-vapor laser lock (DAVLL) [25]. The details of the apparatus design and construction are described in [26]. To produce the two optical fields required for CPT, we combined the direct laser current with a 6.8347 GHz modulation signal produced by the homemade tunable microwave source described below. For most of the data described below, the unmodulated laser frequency (carrier) was tuned at or near $5S_{1/2}F=2\rightarrow 5P_{1/2}F'=1$ transition, while the +1 modulation sideband frequency was correspondingly tuned to $5S_{1/2}F=1\rightarrow 5P_{1/2}F'=1$ transition. We monitored the intensity ratio between the sideband and the carrier using a high-finesse Fabry–Perot cavity with a free spectral range of approximately 40 GHz (not shown in the diagram), and we were able to adjust it in a wide range (from zero to more than 100%) by changing the rf power sent to the VCSEL.

The laser beam with a maximum total power of 120 μW and a slightly elliptical Gaussian profile [1.8 mm and 1.4 mm full width at half-maximum (FWHM)], was linearly polarized by a polarizing beam splitter (PBS) and then directed into the cylindrical Pyrex cell (length 75 mm; diameter 22 mm) containing isotopically enriched ^{87}Rb vapor and 15 Torr of Ne buffer gas. The cell was mounted inside a three-layer magnetic shielding to reduce stray magnetic fields, and its temperature was actively stabilized at 47.5°C. To lift the degeneracy of the Zeeman sublevels we applied a weak homogeneous longitudinal magnetic field $B\approx 12$ mG produced by a solenoid mounted inside the innermost magnetic shield. A photodiode (PD) placed after the cell detected the total transmitted intensity.

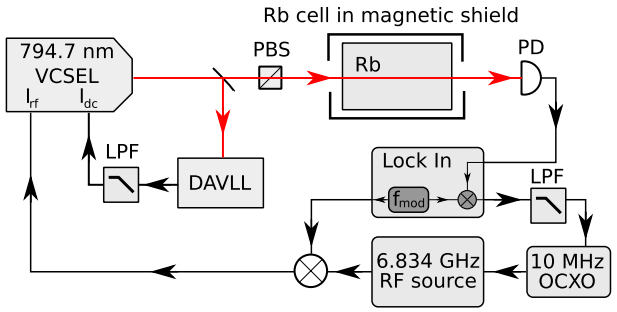

Fig. 2. (Color online) Schematic of the experimental setup. Here PBS is a polarizing beam splitter, LPF is a low-pass filter, PD is a photodetector, and VCOCXO is a voltage-control oven-stabilized oscillator.

In this experiment we used higher buffer gas pressure compared to previous experiments [20,23,24] to extend the diffusion time of atoms through the laser beam (and hence the CPT coherence lifetime) without too much pressure broadening of the optical transitions (≈150 MHz [12]) to maintain good spectral resolution of the two excited states. For a typical miniature atomic clock with cell volume ≈1 mm^3 the buffer gas pressure should be further optimized, since increased buffer gas pressure may result in reduction of a $lin\|lin$ CPT resonance due to the destructive effect of the $F'=2$ excited state.

The detailed schematic of the homemade microwave source operating at 6.835 GHz is shown in Fig. 3. It consists of a Zcomm CRO6835z voltage-control oscillator (VCO) for generation of a microwave field, which is in a phase-locked loop (PLL) with a Wenzel 501-04609 voltage-controlled oven-stabilized 10 MHz crystal oscillator (VCOCXO). A National Semiconductor PLL chip (LMX2487) with a computer-controlled fractional divider allows rough tuning of the microwave frequency with sub-Hz steps in the several-hundreds MHz range, while fine tuning is done via variable voltage of the VCOCXO.

To lock the frequency of the microwave source (and hence the two-photon detuning of the two laser fields) to the maximum transmission, a slow frequency modulation at $f_m=3$ kHz was superimposed on the 6.835 GHz microwave modulation signal. Then the photodetector signal was demodulated at f_m using a lock-in amplifier. The resulting error signal was fed back to lock the frequency of the 10 MHz VCOCXO, and consequently the frequency of the 6.835 GHz signal was phase-locked to the VCOCXO. The frequency of the locked VCOCXO was measured by beating it with a reference 10 MHz signal derived from a commercial atomic frequency standard (SRS FS725).

3. EXPERIMENTAL RESULTS

To determine the optimal parameters for the microwave lock operation, we measured the sensitivity of the clock lock loop (i.e., the slope of the lock-in output error signal) as a function of lock-in frequency and amplitude. The resulting dependence is shown in Fig. 4. Similar to previous studies [27], we found that there is a particular combination of the lock-in parameters that results in the highest slope of the error signal as a function of the two-photon detuning: the lock-in frequency $f_m=3$ kHz, and the modulation depth is 4 kHz. We experimentally confirmed that under these conditions the microwave lock loop is the most sensitive and results in the best frequency stability measurements.

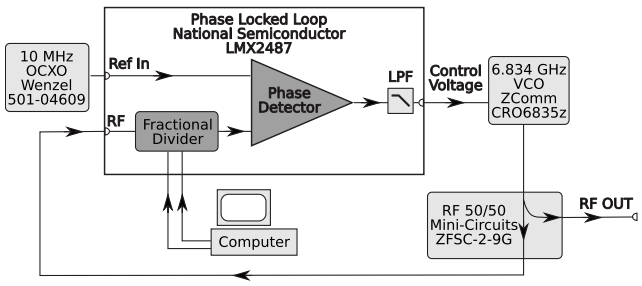

Fig. 3. Schematic of the 6.835 GHz microwave source.

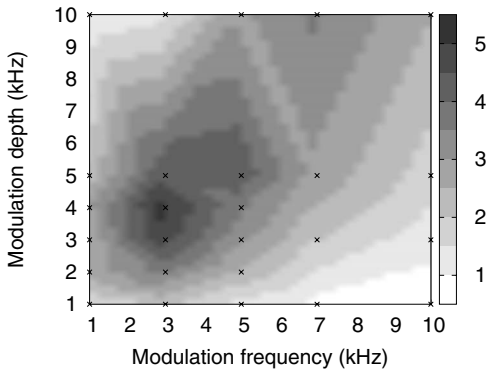

Fig. 4. Dependence of the clock lock loop sensitivity in arbitrary units on the lock-in modulation frequency and modulation depth. Crosses mark measured data points, and the rest of the map is recreated via an interpolation routine.

To ensure stable operation of a CPT-based atomic clock, the frequency of a CPT resonance must be maximally decoupled from any fluctuations of the experimental parameters. For example, any variations in the light intensity change the measured clock frequency because of the resonance light shift due to interaction of various VCSEL modulation components with optical transitions. Since the overall CPT resonance shift combines the contributions of all optical fields on each ground state, it has been previously shown [24] that careful adjustment of the intensity ratio of two CPT optical fields allows cancellation of the first-order light shift. Our current measurements confirm that the same cancellation happens for a current-modulated VCSEL output by adjusting the microwave modulation strength (and hence the sideband/carrier intensity ratio), even though the VCSEL current modulation is not a pure phase modulation as in the case of the electro-optical modulators used in previous studies.

To find the optimal microwave power for light shift cancellation we locked our microwave source on a CPT resonance. We then monitored changes in the oscillator frequency in response to changing the laser power using an acousical-optical modulator (AOM) before the Rb cell. Figure 5 shows measured CPT light shifts for three different strengths of microwave modulation, resulting in 40%,

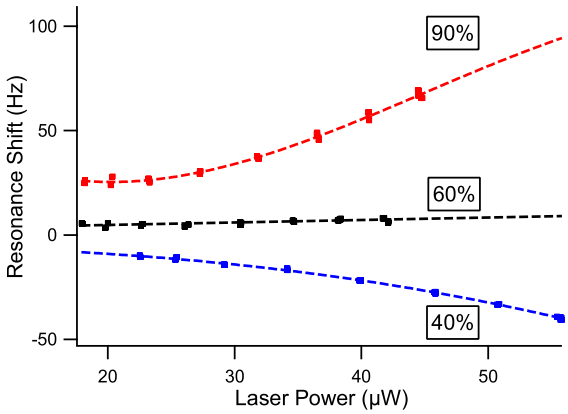

Fig. 5. (Color online) Dependence of the measured clock frequency shift on laser power for three different sideband-carrier ratios (40%, 60%, and 90%). For these measurements the carrier laser frequency was tuned by approximately −200 MHz from $5S_{1/2}F_g=2\rightarrow 5P_{1/2}F_e=1$ transition.

60%, and 90% sideband/carrier intensity ratios. It is clear that the resonance light shift reversed its direction when the modulation power was adjusted from highest to lowest, and for a 60% intensity ratio the CPT resonance frequency was practically independent of the total laser power. We chose this point to operate our clock to minimize the effect of laser intensity fluctuations on clock stability.

Long-term stability of our clock measurements was limited by dependence of the CPT resonance frequency on a slowly drifting laser frequency caused by the DAVLL temperature dependence. To minimize this effect, we studied the CPT resonance shift as a function of the laser one-photon detuning Δ. Figure 6(a) shows the change in CPT resonance frequency as the carrier laser frequency was detuned to the red of $|F=2\rangle \rightarrow |F'=1\rangle$. From this graph it is easy to see that there is no laser detuning with zero first-order dependence of CPT resonance frequency on Δ. However, a moderate red detuning leads to a weaker variation of the CPT resonance frequency with laser detuning. Thus, we have chosen the "optimal" laser detuning of Δ=−200 MHz for operating our atomic clock prototype to minimize the light-shift dependence on laser frequency without significantly degrading the CPT resonance contrast (7% compared to 9% at the resonance frequency) as shown in Fig. 6(b). We also verified that the value of the noise caused by the FM-to-AM conversion of the broadband VCSEL optical output did not noticeably change within a few hundred MHz around the center of the $|F=2\rangle \rightarrow |F'=1\rangle$ transition.

Figure 7(a) shows total transmitted power through the Rb cell as the microwave frequency (i.e., the two-photon detuning) was scanned around the clock transition at the optimal conditions for the first-order light-shift cancellation (sideband/carrier ration 60%, laser detuning Δ =−200 MHz) in the presence of an ≈12 mG longitudinal magnetic field. Three distinct resonances correspond to a magneto-insensitive *lin*∥*lin* CPT resonance [central peak, created by the fields depicted by solid arrows in Fig. 1(b)] and two additional Zeeman-shifted CPT resonance shifts [two side peaks, caused by the Λ configurations shown in dashed arrows in Fig. 1(b)]. As expected from the theory, the central peak has the highest contrast and the narrowest linewidth, two conditions required for optimal microwave oscillator locking.

Figure 7(b) zooms in on the central *lin*∥*lin* CPT resonance to analyze its lineshape. The resonance was slightly asymmetric due to nonzero one-photon laser detuning [28,29]. In this case the CPT resonance lineshape should be described by a generalized Lorentzian function [30],

$$T(\delta) = 1 + \gamma \frac{A\gamma + B(\delta - \delta_0)}{(\gamma)^2 + (\delta - \delta_0)^2}, \quad (1)$$

where $T(\delta)$ is the total laser transmission through the cell normalized to the background I_{bg} (i.e., the transmitted power at large two-photon detuning away from CPT resonance), δ_0 is a resonance shift, γ is a CPT resonance linewidth measured at half maximum, and A and B are amplitudes of the symmetric and anti-symmetric Lorentzian components, respectively. All of the above parameters are weakly dependent on one-photon detunig Δ. Under the conditions of the first-order light-shift cancellation that we used in our atomic clock, the CPT resonance had the following parameters: resonance width γ=700 Hz, resonance contrast C=6.1% (where the contrast is defined as a ratio between resonance amplitude and background), and the resonance asymmetry B/A=0.29. Figure 7(b) shows that Eq. (1) provides an excellent fit to the experimental lineshape everywhere except for the peak of the resonance, where we observed higher and sharper transmission than predicted by the fit. This occurs as a result of the diffusion of atoms and their repeated interaction with the laser field [31,32], and it can improve atomic clock frequency stability by further increasing the overall resonance contrast [33]. For example, the measured CPT contrast exceeded 7% compared to the 6% given by the Lorentzian fit. Also, it is important to note that the resonant asymmetry is quite small and may lead to only a very weak effect of the resonance position on the lock-in slow-modulation parameters [34].

The estimated fractional stability of the microwave oscillator locked to the CPT resonance is proportional to the quality figure $q=C/2\gamma$—the ratio between the resonance contrast and its FWHM. The measured resonance parameters (C=0.07 and γ=700 Hz) provide the quality factor $q \approx 5 \cdot 10^{-5}$/Hz. This value implies the fractional frequency stability (Allan variance) at the level of $\sigma(\tau) \sim 2 \cdot 10^{-14} \tau^{1/2}$ if limited only by the photon shot noise [35],

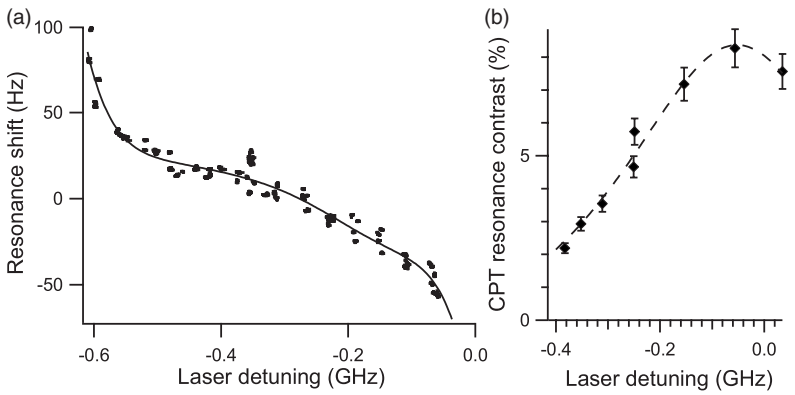

Fig. 6. (a) Measured clock frequency shift and (b) resonance contrast as functions of laser detuning from the $5S_{1/2}F_g=2 \rightarrow 5P_{1/2}F_e=1$ transition. Total laser power is 60 μW, and the sideband-carrier ratio is approximately 50%. Lines are to guide the eye.

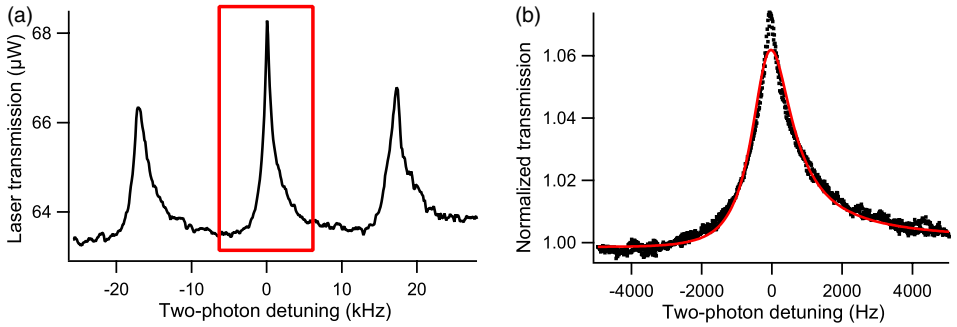

Fig. 7. (Color online) (a) Measured laser power after the Rb cell as a function of the two-photon detuning $\delta - 6.834686890$ GHz in the presence of a constant longitudinal magnetic field $B = 12.3$ mG. The central CPT resonance corresponds to the magnetic-field-insensitive Λ configurations ("clock" transition), shown with bold solid arrows in Fig. 1(b), and two side peaks are magnetic-field-sensitive CPT resonances. Normalized transmission around the central clock resonance is shown (dots) in (b) together with a generalized Lorentzian fit (solid curve). Total input laser power is 120 μW, and all the resonances were recorded under the optimized light-shift cancellation conditions: the sideband-carrier ratio 60%, the carrier laser frequency $\Delta = -200$ MHz.

$$\sigma(\tau) = \frac{1}{4}\sqrt{\frac{\eta e}{I_{\mathrm{bg}} q}}\frac{1}{\nu_0}\tau^{-1/2}. \quad (2)$$

Here $\nu_0 = \Delta_{\mathrm{hfs}} = 6.834$ GHz is the clock reference frequency, e is the electron charge, $\eta = 1.8$ W/A is the photodetector sensitivity (measured optical energy per photoelectron), I_{bg} is the background intensity, and τ is the integration time. However, a broad spectral width of VCSEL results in large residual intensity noise at the output of the cell and therefore significantly degrades realistically achievable frequency stability.

Figure 8 shows the measured fractional Allan deviation of the clock frequency when our prototype CPT clock setup operated at optimal light-shift-cancellation conditions: we detuned our carrier by 200 MHz to decrease sensitivity of the CPT position on the laser detuning (see Fig. 6) and maintained a 60% laser field ratio to eliminate light-shift dependence (see Fig. 5). The short-term stability was $\simeq 2\times 10^{-11}\tau^{-1/2}$ for observation times $1\ \mathrm{s} \leqslant \tau \leqslant 20$ s. This value was most likely limited by the large VCSEL phase noise (≈ 100 MHz) as well as by the stability of our commercial reference clock SRS FS725 with manufacturer fractional stability $<2\times 10^{-11}$ at 1 s. At longer integration times the stability degraded due to uncontrolled temperature variations in our table-top apparatus and their effect on the laser wavelength drift that caused the CPT resonance shift (see Fig. 6). Despite this nonoptimal clock apparatus, the measured short-term frequency stability is already comparable or better than the values reported for many recently demonstrated atomic clocks [1,2,4,36,37]. Our experimental results also match the theoretically predicted stability limited by the broad spectral width of a VCSEL [23]. We expect that both the short- and long-term frequency stability can be further improved with better temperature stabilization of the experimental apparatus, better laser control, and possibly the use of a VCSEL diode with reduced linewidth.

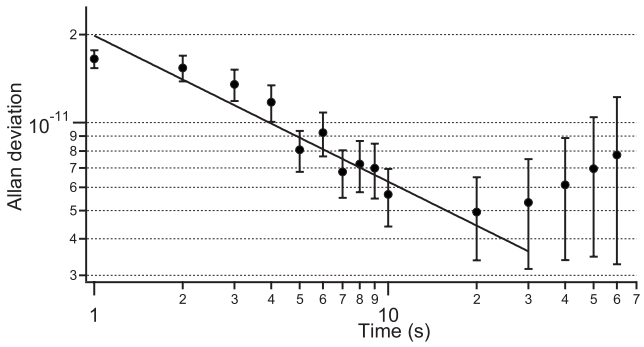

Fig. 8. Measured fractional clock stability of the microwave oscillator locked to the CPT resonance. Solid line shows $\sigma(\tau) = \simeq 2\times 10^{-11}\tau^{-1/2}$ fit.

4. CONCLUSION

In summary, we systematically studied a magneto-insensitive CPT resonance in the *lin*$\|$*lin* configuration using a current-modulated VCSEL on the D_1 line of ^{87}Rb, and identified the optimal parameters for atomic clock operation that cancel the effect of the first-order light shift. Employing this light-shift cancellation in a table-top apparatus (not engineered for stable clock performance), we nonetheless observed short-term frequency stability of $\simeq 2\times 10^{-11}\tau^{-1/2}$ that is comparable to or better than existing CPT clocks. Significant improvements in such clock frequency stability should be possible in a small-scale device with standard techniques minimizing the impact of the environment.

ACKNOWLEDGMENTS

The authors thank Sergey Zibrov for advice on the experimental apparatus design, Chris Carlin for helping with the laser lock construction, and Valery Yudin for useful discussions. This research was supported by Jeffress Research grant J-847 and the National Science Foundation (NSF) grant PHY-0758010.

REFERENCES

1. J. Vanier, "Atomic clocks based on coherent population trapping: a review," Appl. Phys. B: Lasers Opt. **81**, 421–442 (2005).
2. M. Merimaa, T. Lindwall, I. Tittonen, and E. Ikonen, "All-optical atomic clock based on coherent population trapping in ^{85}Rb," J. Opt. Soc. Am. B **20**, 273–279 (2003).

3. S. Knappe, L. Liew, V. Shah, P. Schwindt, J. Moreland, L. Hollberg, and J. Kitching, "A microfabricated atomic clock," Appl. Phys. Lett. **85**, 1460–1462 (2004).
4. S. Knappe, P. D. D. Schwindt, V. Shah, L. Hollberg, J. Kitching, L. Liew, and J. Moreland, "A chip-scale atomic clock based on ^{87}Rb with improved frequency stability," Opt. Express **13**, 1249–1253 (2005).
5. R. Lutwak, J. Deng, W. Riley, M. Varghese, J. Leblanc, G. Tepolt, M. Mescher, D. K. Serkland, K. M. Geib, and G. M. Peake, "The chip-scale atomic clock—low-power physics package," in Proceedings of the 36th Annual PTTI Meeting (2004), pp. 339–354.
6. I. K. Kominis, T. W. Kornack, J. C. Allred, and M. V. Romalis, "A subfemtotesla multichannel atomic magnetometer," Nature **422**, 596–599 (2003).
7. T. W. Kornack, R. K. Ghosh and M. V. Romalis, "Nuclear spin gyroscope based on an atomic comagnetometer," Phys. Rev. Lett. **95**, 230801 (2005).
8. V. Shah, S. Knappe, P. D. D. Schwindt, and J. Kitching, "Subpicotesla atomic magnetometry with a microfabricated vapor cell," Nat. Photonics **1**, 649–652 (2007).
9. M. P. Ledbetter, I. M. Savukov, D. Budker, V. Shah, S. Knappe, J. Kitching, D. J. Michalak, S. Xu, and A. Pines, "Zero-field remote detection of NMR with a microfabricated atomic magnetometer," Proc. Natl. Acad. Sci. U.S.A. **105**, 2286–2290 (2008).
10. W. C. Griffith, R. Jimenez-Martinez, V. Shah, S. Knappe, and J. Kitching, "Miniature atomic magnetometer integrated with flux concentrators," Appl. Phys. Lett. **94**, 023502 (2009).
11. M. Fleischhauer, A. Imamoglu, and J. P. Marangos, "Electromagnetically induced transparency: optics in coherent media," Rev. Mod. Phys. **77**, 633–673 (2005).
12. M. Erhard and H. Helm, "Buffer-gas effects on dark resonances: theory and experiment," Phys. Rev. A **63**, 043813 (2001).
13. S. Knappe, L. Hollberg, and J. Kitching, "Dark-line atomic resonances in submillimeter structures," Opt. Lett. **29**, 388–390 (2004).
14. N. Cyr, M. Têtu, and M. Breton, "All-optical microwave frequency standard: a proposal," IEEE Trans. Instrum. Meas. **42**, 640–649 (1993).
15. Y. Y. Jau, A. B. Post, N. N. Kuzma, A. M. Braun, M. V. Romalis, and W. Happer, "Intense, narrow atomic-clock resonances," Phys. Rev. Lett. **92**, 110801 (2004).
16. A. V. Taichenachev, V. I. Yudin, V. L. Velichansky, S. V. Kargapoltsev, R. Wynands, J. Kitching, and L. Hollberg, "High-contrast dark resonances on the D-1 line of alkali metals in the field of counterpropagating waves," JETP Lett. **80**, 236–240 (2004).
17. Y.-Y. Jau, E. Miron, A. B. Post, N. N. Kuzma, and W. Happer, "Push-pull optical pumping of pure superposition states," Phys. Rev. Lett. **93**, 160802 (2004).
18. T. Zanon, S. Guerandel, E. de Clercq, D. Holleville., N. Dimarcq, and A. Clarion, "High-contrast Ramsey fringes with coherent population trapping pulses in a double lambda atomic system," Phys. Rev. Lett. **94**, 193002 (2005).
19. V. Shah, S. Knappe, L. Hollberg, and J. Kitching, "High-contrast coherent population trapping resonances using four-wave mixing in Rb-87," Opt. Lett. **32**, 1244–1246 (2007).
20. A. V. Taichenachev, V. I. Yudin, V. L. Velichansky, and S. A. Zibrov, "On the unique possibility if significantly increasing the contrast of dark resonances on the D1 line of ^{87}Rb," JETP Lett. **82**, 398–403 (2005).
21. G. Kazakov, B. Matisov, I. Mazets, G. Mileti, and J. Delporte, "Pseudoresonance mechanism of all-optical frequency-standard operation," Phys. Rev. A **72**, 063408 (2005).
22. S. A. Zibrov, V. L. Velichansky, A. S. Zibrov, A. V. Taichenachev, and V. I. Yudin, "Experimental investigation of the dark pseudoresonance on the D1 line of the Rb87 atom excited by a linearly polarized field," JETP Lett. **82**, 477–481 (2005).
23. E. Breschi, G. Kazakov, R. Lammegger, G. Mileti, B. Matisov, and L. Windholz, "Quantitative study of the destructive quantum-interference effect on coherent population trapping," Phys. Rev. A **79**, 063837 (2009).
24. A. S. Zibrov, V. L. Velichansky, A. V. Taichenachev, and V. I. Yudin, "Coherent population trapping resonances with linearly polarized light for all-optical miniature atomic clocks," Phys. Rev. A **81**, 013833 (2010).
25. V. V. Yashchuk, D. Budker, and J. R. Davis, "Laser frequency stabilization using linear magneto-optics," Rev. Sci. Instrum. **71**, 341–346 (2000).
26. N. Belcher, E. E. Mikhailov, and I. Novikova, "Atomic clocks and coherent population trapping: experiments for undergraduate laboratories," Am. J. Phys. **77**, 988–998 (2009).
27. I. Ben-Aroya, M. Kahanov, and G. Eisenstein, "Optimization of FM spectroscopy parameters for a frequency locking loop in small scale CPT based atomic clocks," Opt. Express **15**, 15060–15065 (2007).
28. A. V. Taichenachev, V. I. Yudin, R. Wynands, M. Stahler, J. Kitching, and L. Hollberg, "Theory of dark resonances for alkali vapors in a buffer-gas cell," Phys. Rev. A **67**, 033810 (2003).
29. E. E. Mikhailov, I. Novikova, Y. V. Rostovtsev, and G. R. Welch, "Buffer-gas induced absorption resonances in Rb vapor," Phys. Rev. A **70**, 033806 (2004).
30. S. Knappe, M. Stahler, C. Affolderbach, A. V. Taichenachev, V. I. Yudin, and R. Wynands, "Simple parametrization of dark-resonance line shapes," Appl. Phys. B: Lasers Opt. **76**, 57–63 (2003).
31. Y. Xiao, I. Novikova, D. F. Phillips, and R. L. Walsworth, "Diffusion-induced Ramsey narrowing," Phys. Rev. Lett. **96**, 043601 (2006).
32. Y. Xiao, I. Novikova, D. Phillips, and R. L. Walsworth, "Repeated interaction model for diffusion-induced Ramsey narrowing," Opt. Express **16**, 14128–14141 (2008).
33. I. Novikova, Y. Xiao, D. F. Phillips, and R. L. Walsworth, "EIT and diffusion of atomic coherence," J. Mod. Opt. **52**, 2381–2390 (2005).
34. D. F. Phillips, I. Novikova, C. Y.-T. Wang, M. Crescimanno and R. L. Walsworth, "Modulation induced frequency shifts in a coherent-population-trapping-based atomic clock," J. Opt. Soc. Am. B **22**, 305–310 (2005).
35. J. Vanier, M. W. Levine, D. Janssen, M. J. Delaney, "On the use of intensity optical pumping and coherent population trapping techniques in the implementation of atomic frequency standards," IEEE Trans. Instrum. Meas. **52**, 822–831 (2003).
36. I. Novikova, D. F. Phillips, A. S. Zibrov, R. L. Walsworth, A. V. Taichenachev, and V. I. Yudin, "Cancellation of light shifts in an N-resonance clock," Opt. Lett. **31**, 622–624 (2006).
37. http://www.kernco.com/pdfs/CPT-C01DataSheet060704D.pdf.